Modeling Sex Differences in Pharmacokinetics, Pharmacodynamics, and Disease Progression Effects of Naproxen in Rats with Collagen-Induced Arthritis

Xiaonan Li, Debra C DuBois, Richard R Almon, William J Jusko

Clinical Pharmacokinetics Laboratory, School of Basic Medicine and Clinical Pharmacy, China Pharmaceutical University, Nanjing, Jiangsu, 211198, China (XL); Department of Pharmaceutical Sciences, School of Pharmacy and Pharmaceutical Sciences, State University of New York at Buffalo, Buffalo, NY, 14214, USA (XL, DCD, RRA, WJJ); Department of Biological Sciences, State University of New York at Buffalo, Buffalo, NY, 14260, USA (DCD, RRA)

1

DMD # 74526

Running title: Naproxen Kinetics and Effects in Arthritis

Corresponding author:

William J Jusko, Ph.D.

Department of Pharmaceutical Sciences

School of Pharmacy and Pharmaceutical Sciences

State University of New York at Buffalo

Buffalo, NY, 14214

Telephone: 716-645-2855

Fax: 716-829-6569

E-mail: wjjusko@buffalo.edu

Number of text pages: 14

Number of tables: 2

Number of figures: 4

Number of references: 46

Number of words:

Abstract: 247

Introduction: 608

Discussion: 1504

ABBREVIATIONS: CIA, collagen-induced arthritic; COX, cyclooxygenase; CV, coefficient of variation; IP, intraperitoneally; ISF, interstitial fluid; PBPK, physiologically based pharmacokinetic; mPBPK, minimal PBPK; NPX, Naproxen; NSAIDs, nonsteroidal anti-inflammatory drugs; PK/PD, pharmacokinetics and pharmacodynamics; PG, prostaglandins; RA, rheumatoid arthritis; SF, synovial fluid; 2CM, two-compartment model.

DMD # 74526

ABSTRACT

Naproxen (NPX) is a frequently used nonsteroidal anti-inflammatory drug (NSAID) for rheumatoid arthritis (RA). Lack of quantitative information about the drug exposure-response relationship has resulted in empirical dosage regimens for use of NPX in RA. Few studies included sex as a factor, although RA predominates in women. A pharmacokinetic, pharmacodynamic, and disease progression (PK/PD/DIS) model described the anti-inflammatory effects of NPX in collagen-induced arthritic (CIA) male and female rats. Three groups of rats were included for each sex: healthy animals, CIA controls, and CIA rats given 50 mg/kg single dose NPX intraperitoneally (IP). Paw volumes of healthy rats indicated natural growth and disease status was measured by paw edema. An innovative minimal physiologically based pharmacokinetic (mPBPK) model incorporating nonlinear albumin binding of NPX in both plasma and interstitial fluid (ISF) was applied. Arthritic rats exhibited lower plasma and ISF albumin concentrations and reduced clearances of unbound drug to explain PK profiles. The unbound ISF NPX concentrations predicted by the mPBPK model were used as the driving force for pharmacological effects of NPX. A logistic growth function accounting for natural paw growth and an indirect response model for paw edema and drug effects (inhibition of k_{in}) was applied. Female rats showed higher incidence of CIA, earlier disease onset, and more severe symptoms. NPX had stronger effects in males owing to higher unbound ISF NPX concentrations and lower IC_{50} values. The model described the PK, unbound NPX in ISF, time-course of anti-inflammatory effects, and sex differences in CIA rats.

Introduction

Rheumatoid arthritis (RA), a chronic systemic inflammatory autoimmune disease, affects nearly 1% of adults world-wide and significantly reduces health-related quality of life. The pathogenesis of RA involves a complex interplay between both environmental and genetic factors, leading to the infiltration of immune cells and increased production of various pro-inflammatory mediators such as cytokines and prostaglandins (PG) in joints (McInnes and Schett, 2011). In particular, PG play an important role in the generation of typical inflammatory responses such as pain, fever, redness and swelling through local vasodilation and amplification of cytokine signaling (Funk, 2001; Ricciotti and FitzGerald, 2011; Aoki and Narumiya, 2012). Therefore, PG signaling has been a major therapeutic target of RA.

Naproxen (NPX), a traditional nonsteroidal anti-inflammatory drug (NSAID), has been extensively used in the long-term treatment of RA and other joint diseases because of its rapid relief of inflammatory symptoms and well-tolerated adverse effects (Watson et al., 2002). Similar to other NSAIDs, NPX exerts its anti-inflammatory effects mainly through the inhibition of cyclooxygenase (COX) activity and directly blocks the formation of PG at sites of inflammation, thereby suppressing the inflammatory responses (Vane, 1971; Crofford, 2013). However, dosing regimens for NPX in treating RA have been empirical due to the lack of convincing information on the relationship between drug exposure and clinical response. The NPX concentration–response relationship in RA was explored (Dunagan et al., 1988; Day et al., 1995), but only a trend was obtained and the pharmacokinetics and pharmacodynamics (PK/PD) of NPX were not quantitatively analyzed. Recent studies (Huntjens et al., 2006; Huntjens et al., 2010) assessed the correlation between *in vitro* and *in vivo* exposure-effect relationships of NPX as well as the impact of chronic inflammation on the PK/PD of NPX. However, the nonlinear PK behavior of NPX was not considered. Other studies merely described the nonlinear exposures of NPX in acute inflammation (Josa et al., 2001; Krekels et al., 2011). The clinical efficacy of NPX appeared to be better correlated with its unbound concentrations in synovial fluid (SF) as synovium is the proposed site of action in RA (Jalava et al., 1977; Netter et al., 1989; Bertin et al., 1994; Day et al., 1995). In spite of this literature, there are limited quantitative insights into the PK/PD relationships of NPX in chronic inflammatory conditions such as RA.

Similar to other autoimmune diseases, RA predominates in women (Jawaheer et al., 2006; van Vollenhoven, 2009). However, very few preclinical studies include sex as a factor in PK/PD. Most studies were carried out in males, with little information available on potential sex differences in drug action in RA.

The collagen-induced arthritic (CIA) rat model is the most frequently used animal model for RA, and mimics many disease characteristics of human RA (Stuart et al., 1982; Holmdahl et al., 2001). The impact of sex and RA on the PK of NPX was assessed using this animal model, where concentration-dependent binding was incorporated into a two-compartment model (2CM) to account for the nonlinearity and disease effects of NPX PK (Li et al., 2017). However, there are advantages to be gained by use of an extended minimal physiologically-based pharmacokinetic (mPBPK) model for describing the PK of NPX, particularly for describing unbound NPX in interstitial fluid (ISF) and SF, adjacent to the site of action.

This study has two purposes. One is to assess and validate a proposed mPBPK model for quantitating the PK of unbound NPX in normal and CIA male and female rats and provide the biophase concentrations. The second is to develop a PK/PD disease (DIS) model for evaluation of the time course of disease progression and anti-inflammatory effects of NPX in male and female CIA rats.

Materials and Methods

Animals. Male and female Lewis rats (5-8 weeks old) were purchased from Harlan (Indianapolis, IN), weighing approximately 110 to 160 g for females and 170 to 220 g for males, age-matched for each sex group at the time of PK/PD studies. Care of animals, induction of arthritis, measurements of paw edema, and other experimental details are presented in our companion manuscript (Li et al., 2017).

Drug. The sodium salt of NPX (N51601) was obtained from Sigma-Aldrich Inc. (St. Louis, MO). The NPX working stocks were freshly prepared as a sodium NPX solution in phosphate buffered saline (PBS) (pH=8), and filtered through 0.22 micron filters before use. The drug was administered IP in a volume of 1 mL/kg.

Experimental Design. Hind paw swelling was used as the indicator for edema. Two cross-sectional areas of the paw were measured by digital calipers (VWR Scientific, Rochester, NY) as previously described (Earp et al., 2008).

Pilot studies showed that peak edema without drug treatment was observed on day 16 for females and day 21 for males. Rats with a paw volume increase of at least 50% in one or both hind paws were considered to be arthritic after evaluation on day 15 for females and day 20 for males. Eight female CIA and 8 male CIA rats were selected and randomly divided into two subgroups per sex: vehicle control groups (n=4) receiving only IP PBS; treatment groups (n=4) which received 50 mg/kg IP NPX. Control or treatment groups received injections on day 16 for females and day 21 for males. The hind paws of 4 healthy females and 4 healthy males were measured through the entire study to obtain the natural paw growth. Paw edema and body weights were monitored before disease induction (day 0) and post-induction on days 3, 7, 9, 10, 11, 13, 14, and 15 for both sex groups and 17 to 20 days for CIA males. Starting from the dosing day, paw edema was measured before dosing and at 1, 2, 4, 6, 8, 12, 24 and 36 h after dosing and on post-dose days 3, 4, 5, 6, 7, 8, 9 and 10.

Serial blood samples were collected from the saphenous vein at 15, 30 and 45 min and 1, 2, 4, 6, 9, 12, 24 h post-dose and processed and analyzed for NPX by LC-MS/MS as described by Li et al. (2017).

Pharmacokinetic Model. The extended mPBPK model with plasma and one tissue compartment

is shown in Figure 1. The differential equations for the PK are:

$$\frac{dA_a}{dt} = -k_a \cdot A_a, \qquad\qquad A_a(0) = F \cdot \text{Dose} \qquad\qquad (1)$$

$$V_p \cdot \frac{dC_p}{dt} = k_a \cdot A_a + f_d \cdot Q_{co} \cdot (C_{ut} - C_{up}) - CL_{up} \cdot C_{up}, \qquad C_p(0) = 0 \qquad\qquad (2)$$

$$V_t \cdot \frac{dC_t}{dt} = f_d \cdot Q_{co} \cdot (C_{up} - C_{ut}), \qquad\qquad C_t(0) = 0 \qquad\qquad (3)$$

where A_a indicates the amount of NPX at the absorption site, k_a is the first-order absorption rate constant,

C_p and C_t are total NPX concentrations in V_p (plasma volume) and V_t (ISF volume), Q_{co} is cardiac output

plasma flow, f_d is the fraction of Q_{co} that perfuses V_t, CL_{up} is clearance of unbound NPX from plasma,

C_{up} and C_{ut} are the unbound NPX concentrations in plasma and ISF, and F is the bioavailability of the IP

dose calculated to be about 0.9 from literature intravenous data in rats (Lauroba et al., 1986). The

physiological restrictions of relevant parameters are:

$$f_d \leqslant 1 \text{ and } V_p + V_t = \text{Extracellular Fluid Volume (ECF = 206.29 mL/kg) (Shah and Betts, 2012)}$$

In order to account for the nonlinearity of NPX PK, the model incorporated nonlinear protein

binding in both plasma and ISF. The unbound concentrations in both plasma and ISF were calculated from

measurements of total NPX, albumin concentrations, and binding parameters obtained using ultrafiltration

as described in our companion manuscript (Li et al. 2017):

$$C_u = (-(n_1 Pt \cdot K_{a1} + n_2 Pt \cdot K_{a2} - C_t \cdot K_{a1} + 1) +$$

$$\sqrt{4 \cdot (n_2 Pt \cdot K_{a2} \cdot K_{a1} + K_{a1}) \cdot C_p + (n_1 Pt \cdot K_{a1} + n_2 Pt \cdot K_{a2} - C_p \cdot K_{a1} + 1)^2}) / 2 \cdot (n_2 Pt \cdot K_{a2} \cdot K_{a1} +$$

$$K_{a1}) \qquad\qquad (4)$$

where C_u and C_t are the unbound and total drug concentrations in plasma or ISF, Ka_1 and Ka_2 are the

association constants for the first and second class of binding sites, n_1 and n_2 are the numbers of first and

second class of binding sites, and Pt is albumin concentration in plasma or ISF.

Several PK modeling assumptions were made: (1) The distribution and elimination processes

operate only on free drug. (2) Penetration of NPX into cells is expected to be minimal (Poulin, 2015), thus

the distribution of NPX is restricted to plasma and ISF. (3) The concentration-dependent binding of NPX

is limited to albumin in both plasma and ISF. (4) The binding affinity of NPX to albumin is the same in

both plasma and ISF in all animals. (5) The ratio of ISF-to-plasma albumin concentration is 0.5 for healthy

rats and 0.9 for CIA rats (Li et al, 2017). The unbound NPX concentrations in ISF were calculated using

the final PK model parameters and used as the driving force for PD effects in CIA rats.

This model was confirmed as relevant by comparing observed PK data for NPX in plasma and ISF

from a study where plastic sponges were implanted subcutaneously into each animal to suck up the

inflammatory exudate and NPX concentrations in the exudate were measured as the ISF concentrations.

These data were digitized from the literature (Doherty et al., 1977; Huntjens et al., 2006) with the model-

predicted concentration-time profiles. Also, data for total and unbound naproxen concentrations in plasma

and SF from human subjects (Day et al, 1999) were compared.

Pharmacodynamics and Disease Progression Model. Three different models were tested and

compared for fitting the disease progression profiles for paw edema with and without NPX treatment. The

first model was a transduction-based feedback model which consisted of a series of transit compartments

accounting for both the production and natural remission of paw edema (Liu et al., 2011). The second was

an indirect response model containing zero-order natural growth combined with a feedback on the

production of paw edema (Lon et al., 2013). The third model applied a logistic growth function to describe

the natural growth of paw instead of a zero-order growth parameter. The final model equations and initial

conditions are:

$$\frac{dPaw}{dt} = \begin{cases} k_g \cdot Paw \cdot \left(1 - \frac{Paw}{Paw_{ss}}\right), & t < t_{onset} \\ k_g \cdot Paw \cdot \left(1 - \frac{Paw}{Paw_{ss}}\right) + k_{in}(t) \cdot \left(1 - \frac{I_{max} \cdot C_{ut}}{IC_{50} + C_{ut}}\right) - k_{out} \cdot Paw, & t \geq t_{onset} \end{cases} \quad Paw(0) =$$

$$Paw^0 \tag{5}$$

$$\frac{dk_{in}}{dt} = -k_{deg} \cdot k_{in}, \qquad\qquad k_{in}(0) = k_{in}^0 \tag{6}$$

where Paw is the sum of ankle and paw areas of a rat hind foot; Paw^0 is the paw size on day 0; Paw_{ss} is

the normal paw size at steady-state; k_g is the natural growth rate constant of paw in healthy rats; t_{onset} is

the time delay observed before disease onset; $k_{in}(t)$ is a function of time and represents the production of

paw edema after disease onset; k_{in}^0 is the production rate constant of paw edema at t_{onset}; and k_{deg} is a

linear decline in k_{in} accounting for the natural remission of arthritis; drug-related parameters I_{max} and

IC_{50} are the maximum inhibition effect of NPX on paw edema and NPX concentration at 50% of maximum

inhibition.

Modeling Fitting and Data Analysis. Model fittings were performed by nonlinear regression

using the maximum likelihood algorithm in ADAPT 5 (D'Argenio et al., 2009). The model code is provided

in the Supplementary Materials. All PK data from Li et al. (2017) and PD data from this study were naive-

pooled before analysis. The PK profiles were first fitted and the estimated PK parameters were fixed and

used in the PK/PD model. The variance model used was:

$$V_i = (\sigma_1 + \sigma_2 \cdot Y_i)^2 \tag{7}$$

where V_i represents the variance of the ith data point and Y_i is the ith model-predicted plasma concentration,

and σ_1 and σ_2 are variance model parameters that were estimated together with other system parameters

during model fitting. Model selection was based on the goodness-of-fit criteria which included the Akaike

Information Criterion (AIC), visual inspection of the fitted profiles, and Coefficients of Variation (CV%)

of the parameter estimates. Statistical analysis of paw measurements were performed by Student's *t*-test

using SPSS software version 22 (IBM SPSS Statistics, Chicago, IL), and $p < 0.05$ was considered to be

statistically significant.

Results

Pharmacokinetics

The final PK/PD model is displayed in Figure 1. The mPBPK model features utilization of a physiological structure along with parameters (V_p, V_{ISF} and Q_{co}) applicable to rats, obtained from the literature (Shah and Betts, 2012), and fixed in the model fitting. Concentration-dependent protein binding in both plasma and ISF based on our measurements were incorporated into the basic mPBPK model to account for the nonlinearity of NPX PK. All PK data from our previous study (Li et al., 2017) were modeled simultaneously with different albumin concentrations and unbound clearance terms assigned to arthritic versus healthy rats (Supplemental model code for PK estimation). The PK profiles of total NPX after giving 50 mg/kg IP doses to female and male arthritic rats and the model fittings are shown in Figure 2 (A and B). The PK parameter estimates are listed in Table 1. As can be seen from these results, this model described the PK data well with reasonable CV% for the estimated parameters. The absorption of NPX from the IP injection site was rapid ($k_a \approx 1$ h^{-1}). Arthritic rats showed lower unbound plasma clearance of NPX (1438 mL/h/kg) compared with healthy rats (1968 mL/h/kg), which is in accordance with findings in humans (van den Ouweland et al., 1987). The estimated tissue distribution rate of NPX was much lower ($f_d = 0.15$) than the cardiac plasma flow (when $f_d = 1$), which is in line with the permeability-limited distribution of NPX as it is a highly protein-bound drug.

Figure 2 (C to F) illustrates the model-predicted total and unbound NPX concentrations in both plasma and ISF in male and female CIA rats after 50 mg/kg IP dosing (Supplemental model code for PK simulation 1). The peak concentrations of total and unbound NPX in plasma are greater than those in ISF. The distribution of NPX into and out of tissues is relatively slow resulting in more sustained tissue concentrations compared with the PK profiles in plasma. As shown in the embedded figure in Figure 2, unbound ISF NPX concentrations are slightly higher in males than females, which is accounted for in the model fittings by the lower albumin concentrations in male ISF.

Model simulations using the PK parameters listed in Table 1 overlaid with literature-reported NPX concentration-time profiles in plasma and presumed ISF from rats are displayed in Figure 3 (Supplemental

model code for PK simulation 2 and 3). The model predictions agree well with these independent

experimental PK data, with close predictions of NPX concentrations for a range of doses in these two

studies. Further, direct measurements of total and unbound plasma and SF concentrations of naproxen in

subjects given single doses (Bertin et al, 1994) and multiple oral doses (Day et al, 1999) exhibit profiles

closely resembling those shown in Figure 2 with total and unbound SF concentrations being much lower

than plasma concentrations with a similar later peak and longer persistence than in plasma.

Pharmacodynamics and Disease Progression. Natural growth of paws in healthy rats, disease

progression of paws in control and NPX-treated CIA rats, and the model fittings are shown in Figure 4.

After collagen induction, a typical pattern of paw edema progression without treatment features a delayed

disease onset, rapid rise to peak disease status, and a later slow remission phase. There was no significant

difference ($P > 0.05$) in paw volume of CIA rats among all groups before drug or placebo dosing (day 16

for females and day 21 for males). A significant reduction of paw edema ($P < 0.05$) was observed in both

female and male arthritic rats one day after a single dose of NPX compared with control CIA rats.

With model-predicted unbound NPX concentrations in ISF (Figure 2) used as the driving force for

the PD effects, the model was able to simultaneously characterize the paw volume-time profiles of all

groups very well (Supplemental model code for PD estimation). The final PD/DIS parameter estimates are

summarized in Table 2. All parameters were well estimated with acceptable CV% values. A logistic

function was applied to describe the natural growth of the paw before disease onset (days 0-11 for females

and days 0-13 for males), the gradual increase in paw sizes in both healthy and CIA rats was well captured

and the natural growth rate constant (k_g) was estimated to be 0.003 h^{-1} for females and 0.002 h^{-1} for males.

Sex differences were seen in the paw edema disease progression in CIA rats. The disease onset was

earlier and incidence higher in female as compared to male CIA Lewis rats. This is in agreement with RA

findings in humans (van Vollenhoven, 2009). The estimated t_{onset} value for female arthritic rats (289 h) was

smaller than that for males (308 h), which is close to the male values reported previously (Earp et al., 2009;

Lon et al., 2011; Lon et al., 2013). The induction rate of arthritis was higher in females (80%) than in males

(60%) and the maximum paw size increase was approximately 2-fold for females and 1.7-fold for males

11

compared with healthy controls. The disease production rate constant at t_{onset} (k_{in0}) was about 2.2 mm^2/h for females and 1.4 mm^2/h for males, which is consistent with the clinical evidence that females have greater immune reactivity (Cutolo et al., 2004b). The loss of production rate constant k_{deg} was estimated to be 0.001 h^{-1} for both sex groups. The loss of edema rate constant (k_{out}) was estimated to be 0.007 h^{-1} for males, comparable to our previous value (0.005 h^{-1}) (Lon et al., 2011), while the k_{out} for females was estimated to be 0.013 h^{-1}.

The anti-inflammatory effects of NPX in CIA rats also exhibited sex differences. The maximum effect of NPX on paw edema (I_{max}) was 0.75 for females and 1.0 for males. Preliminary fittings allowing the I_{max} for male rats to vary yielded an estimate that was larger than 1. I_{max} is the maximum fractional extent of inhibition with an upper limit of 1 and thus was set as 1 in our final model fittings. The IC_{50} of NPX was larger in females (0.221 µg/mL) compared to that in males (0.136 µg/mL). These results indicate that the single doses of NPX have moderate but significant anti-inflammatory effects on paw edema in both sex groups and with slightly more potency in males, which occurs in concert with the higher unbound NPX concentrations in ISF of male arthritic rats (Figure 2).

Discussion

Pharmacokinetics of NPX. In our previous study, the nonlinear PK of a range of doses of NPX was explored with comparisons based on sex and presence of RA, where a 2CM incorporating nonlinear binding was applied (Li et al., 2017). This model was an extension of a published 2CM that included only linear protein binding and it functioned reasonably well for addressing major PK issues such as sex and RA. However, there is limited physiologic relevance in such models. The PK parameters depend only on the quality of the PK data and have ambiguous biological features regarding tissue distribution. Drug concentrations outside of plasma, especially when protein binding is nonlinear, cannot be reasonably predicted using a 2CM where the peripheral volume is an apparent parameter with unclear physiological relevance. Nevertheless, compartmental models are extensively used in PK and reasonably capture measured plasma concentrations (Huntjens et al, 2006). The mPBPK model has physiological and anatomical properties, with drug specificity added in consideration of nonlinear protein binding and expectations that ionized weak acids such as NSAIDs distribute primarily in plasma and ISF (Cao and Jusko, 2012). With various assumptions made, the model allows calculation of NPX concentrations in ISF. These were verified by assessment of directly measured PK profiles observed in ISF and SF in the literature. Both the 2CM and mPBPK models allowed a global analysis of all PK data over a range of doses simultaneously, showed that differing albumin concentrations accounted for most of the sex and disease differences, and that RA produced a lower clearance of unbound NPX.

Like all NSAIDs, NPX is a weak acid (pKa = 4.15), which is highly ionized (fraction ionized > 0.99) at physiological pH. Owing to the pH differences between ECF (pH 7.4) and cell water (pH 7.0), NPX is probably localized mainly in the extracellular space with negligible cell water distribution (Poulin, 2015). The reported small volume of distribution (about 0.14 L/kg) supports this (Day et al., 1995). Therefore, ISF was assigned as the tissue space for NPX. Again, as with most NSAIDs, NPX shows extensive and strong binding to plasma proteins at therapeutic concentrations (>99%), with binding predominantly to albumin (Mortensen et al., 1979). Somewhat less binding was found in ISF and tissues due to lower protein concentrations (Wanwimolruk et al., 1983; Day et al., 1995). It was demonstrated

13

previously that nonlinear protein binding of NPX also occurs in synovial fluid in addition to plasma (Day et al., 1995). Thus, concentration-dependent binding of NPX to albumin in both plasma and ISF were components of the mPBPK model.

In a basic mPBPK model, the partition coefficient (K_p) is a constant that must be estimated when total drug concentrations are used with linear binding. Since K_p reflects the ratio of unbound plasma (f_{up}) to unbound tissue (f_{ut}) binding, there is no K_p in the current PK model because such binding was already accounted for. According to the traditional view $K_p = f_{up}/f_{ut}$; here K_p is not a constant but changes with time and total drug concentrations.

The estimated f_d value for NPX was much smaller than 1 (Table 1), indicating that the distribution rate of unbound NPX into tissues was much lower than cardiac output plasma flow and thus mainly controlled by permeability. The comparable parameter in a 2CM is distribution clearance, viz $CL_D = f_d \times Q_{co}$.

The clearance of NPX depends primarily on hepatic metabolism through cytochromes CYP2C9 and CYP1A2 (Miners et al., 1996). Thus a lower unbound clearance (CL_{up}) could be expected in arthritic rats since inflammation is associated with reduced CYP activity due to the pro-inflammatory mediators (Slaviero et al., 2003; Renton, 2005). Both the nonlinear 2CM and the present mPBPK model yielded similar values and conclusions regarding the effect of sex and CIA on clearance of unbound NPX.

CIA Model of Arthritis. Sex differences occur in many autoimmune diseases such as RA, with higher prevalence (sex ratio is 3:1), earlier onset, and more severe disease course in women (Linos et al., 1980; Sokka et al., 2009; van Vollenhoven, 2009). Female sex is also a risk factor for a worse outcome with the same treatments (Symmons, 2002). The reasons for such differences are not well understood, but it is likely that genetic factors and hormones play a role. Female estrogens may be involved in RA onset, whereas androgens might play a suppressive role in disease development (Van Vollenhoven and McGuire, 1994; Cutolo et al., 2004a; Cutolo et al., 2004b). In addition, muscle strength of men is better, which might allow for more successful compensation for functional losses (van Vollenhoven, 2009). All these factors are possible contributors to the sex differences in RA.

14

DMD # 74526

The utility of various rat models of arthritis was compared previously (Earp et al., 2009), and the CIA rat model mirrors many aspects of human RA in a relatively short experimental time-frame such as immune cell infiltration, synovial cell proliferation, and bone destruction. Chronic doses of oral NPX were shown to have good efficacy in female CIA rats (Takeshita et al., 1997). In the present study, the effects of single IP doses of NPX were investigated. Paw swelling (edema) in CIA rats, as one of the most important features of RA, was used as the endpoint of interest. The disease progression of CIA rats in our study exhibited similar sex difference characteristics as human RA. Actual paw volumes were fitted in this study, which was preferable to use of relative paw ratios (Earp et al., 2009), because of the size differences of male and female rats.

Pharmacodynamics of NPX. The current PD model consists of a logistic growth function and an indirect response model (IDR). The logistic growth function allowed an upper limit of paw growth to be anticipated, so that the natural growth in healthy rats and the slight initial increase in paw edema in arthritic rats could be characterized realistically. The paw size increase in CIA rats was attributed to both natural paw growth and paw swelling. The parameters k_g and Paw_{ss} were obtained through joint fitting of the paw data from all groups with the logistic growth function. The turnover of paw edema in CIA rats was described by the IDR composed of a zero-order production process (k_{in}) and a first-order dissipation process (k_{out}). The production of paw swelling was triggered by a series of immune responses resulting from infiltration of immune cells to inflamed tissues and synthesis of pro-inflammatory mediators upon recognition of type II porcine collagen as an exogenous stimulus. On the other hand, the anti-inflammatory cytokines such as interleukin (IL)-4 and IL-10 serve as a counterbalance to the activity of pro-inflammatory cytokines resulting in the later reduction of paw edema (k_{out}). A time-dependent change in either generation or loss processes in chronic degenerative diseases such as RA could result in the natural disease remission (Post et al., 2005). Therefore, a linear function k_{deg} was introduced to negatively regulate the disease production k_{in}. Different initial estimates of k_{in} and Paw were assigned to each group considering their intrinsic variation to allow for flexibility in fitting. The inhibition of k_{in} characterized the effects of NPX, which is mechanistically in line with the pharmacology of NPX. The NSAIDs suppress the enzymatic activity of

15

DMD # 74526

COX and directly inhibit the formation of PG that determine inflammatory responses. Therefore, when NPX was added, the drug inhibition parameters (I_{max} and IC_{50}) would cause a decrease in k_{in} producing the observed reduction in paw volumes (Figure 4). Our study demonstrated that a single dose of NPX exerts moderate but significant anti-inflammatory effects on reducing paw edema in both female and male arthritic rats. Males showed better responses as partly attributable to their higher unbound ISF NPX concentrations (Figure 2) and as reflected by their I_{max} and IC_{50} values (Table 2). This is in accordance with findings of NPX effects in humans (Symmons, 2002).

In conclusion, with incorporation of nonlinear binding in both plasma and ISF, the mPBPK model worked well in handling the effects of reduced albumin concentrations, sex, and disease on distribution and disposition of NPX and also confirmed plasma and tissue (ISF, SF) concentrations of NPX in other published studies in rats and man. The PK/PD relationship of NPX could be established more realistically by using ISF unbound concentrations, mimicking the biophase, as the driving force of its PD effects. The mPBPK/PD/DIS model captured the paw volume versus time profiles in both healthy and CIA rats with or without treatment, and further revealed sex differences in natural disease progression and effects of NPX. Future studies might assess a wider range and chronic doses of NPX and seek more physiological and disease-related biomarkers (such as the expression of COX and PG) in paw tissues to allow for the development of more mechanistic insights and advanced PK/PD/DIS models. This study can serve as a basis for better quantitative assessment of both the PK as well as the PD properties of other NSAIDs and aid in designing drug combination studies with other anti-rheumatic drugs to assess possible synergies and improve rational dosing regimens in RA treatment.

16

Authorship contributions

Participated in research design: Li, DuBois, Almon, Jusko

Conducted experiments: Li, DuBois

Performed data analysis: Li, Jusko

Wrote or contributed to the writing of the manuscript: Li, DuBois, Almon, Jusko

References

Aoki T and Narumiya S (2012) Prostaglandins and chronic inflammation. *Trends Pharmacol Sci* **33:**304-311.

Bertin P, Lapicque F, Payan E, Rigaud M, Bailleul F, Jaeger S, Treves R, and Netter P (1994) Sodium naproxen: concentration and effect on inflammatory response mediators in human rheumatoid synovial fluid. *Eur J Clin Pharmacol* **46:**3-7.

Cao Y and Jusko WJ (2012) Applications of minimal physiologically-based pharmacokinetic models. *J Pharmacokinet Pharmacodyn* **39:**711-723.

Crofford LJ (2013) Use of NSAIDs in treating patients with arthritis. *Arthritis Res Ther* **15 Suppl 3:**S2.

Cutolo M, Sulli A, Capellino S, Villaggio B, Montagna P, Seriolo B, and Straub RH (2004a) Sex hormones influence on the immune system: basic and clinical aspects in autoimmunity. *Lupus* **13:**635-638.

Cutolo M, Villaggio B, Seriolo B, Montagna P, Capellino S, Straub RH, and Sulli A (2004b) Synovial fluid estrogens in rheumatoid arthritis. *Autoimmun Rev* **3:**193-198.

D'Argenio D, Schumitzky, A, Wang, X. (2009) Adapt 5 User's Guide: Pharmacokinetic/Pharmacodynamic Systems Analysis Software, BMSR, University of Southern California.

Day RO, Francis H, Vial J, Geisslinger G, and Williams KM (1995) Naproxen concentrations in plasma and synovial fluid and effects on prostanoid concentrations. *J Rheumatol* **22:**2295-2303.

Doherty NS, Anttila M, and Dean PB (1977) Penetration of naproxen and salicylate into inflammatory exudates in the rat. *Ann Rheum Dis* **36:**244-248.

Dunagan FM, McGill PE, Kelman AW, and Whiting B (1988) Naproxen dose and concentration: response relationship in rheumatoid arthritis. *Br J Rheumatol* **27:**48-53.

Earp JC, DuBois DC, Almon RR, and Jusko WJ (2009) Quantitative dynamic models of arthritis progression in the rat. *Pharm Res* **26:**196-203.

Earp JC, DuBois DC, Molano DS, Pyszczynski NA, Keller CE, Almon RR, and Jusko WJ (2008) Modeling corticosteroid effects in a rat model of rheumatoid arthritis I: mechanistic disease progression

model for the time course of collagen-induced arthritis in Lewis rats. *J Pharmacol Exp Ther* **326:**532-545.

Funk CD (2001) Prostaglandins and leukotrienes: advances in eicosanoid biology. *Science* **294:**1871-1875.

Holmdahl R, Lorentzen JC, Lu S, Olofsson P, Wester L, Holmberg J, and Pettersson U (2001) Arthritis induced in rats with nonimmunogenic adjuvants as models for rheumatoid arthritis. *Immunol Rev* **184:**184-202.

Huntjens DR, Spalding DJ, Danhof M, and Della Pasqua OE (2006) Correlation between in vitro and in vivo concentration-effect relationships of naproxen in rats and healthy volunteers. *Br J Pharmacol* **148:**396-404.

Huntjens DR, Spalding DJ, Danhof M, and Della Pasqua OE (2010) Impact of chronic inflammation on the pharmacokinetic-pharmacodynamic relationship of naproxen. *Eur J Pain* **14:**227 e221-210.

Jalava S, Saarimaa H, Anttila M, and Sundquist H (1977) Naproxen concentrations in serum, synovial fluid, and synovium. *Scand J Rheumatol* **6:**155-157.

Jawaheer D, Lum RF, Gregersen PK, and Criswell LA (2006) Influence of male sex on disease phenotype in familial rheumatoid arthritis. *Arthritis Rheum* **54:**3087-3094.

Josa M, Urizar JP, Rapado J, Dios-Vieitez C, Castaneda-Hernandez G, Flores-Murrieta F, Renedo MJ, and Troconiz IF (2001) Pharmacokinetic/pharmacodynamic modeling of antipyretic and anti-inflammatory effects of naproxen in the rat. *J Pharmacol Exp Ther* **297:**198-205.

Krekels EH, Angesjo M, Sjogren I, Moller KA, Berge OG, and Visser SA (2011) Pharmacokinetic-pharmacodynamic modeling of the inhibitory effects of naproxen on the time-courses of inflammatory pain, fever, and the ex vivo synthesis of TXB2 and PGE2 in rats. *Pharm Res* **28:**1561-1576.

Lauroba J, Domenech J, Moreno J, and Pla-Delfina JM (1986) Relationships between biophasic disposition and pharmacokinetic behavior in nonsteroid antiinflammatory drugs. *Arzneimittelforschung* **36:**710-714.

Linos A, Worthington JW, O'Fallon WM, and Kurland LT (1980) The epidemiology of rheumatoid arthritis in Rochester, Minnesota: a study of incidence, prevalence, and mortality. *Am J Epidemiol* **111:**87-98.

Li X, DuBois DC, Almon RR, and Jusko WJ (2017) Effect of disease-related changes in plasma albumin on the pharmacokinetics of naproxen in male and female arthritic rats, Submitted for publication.

Liu D, Lon HK, DuBois DC, Almon RR, and Jusko WJ (2011) Population pharmacokinetic-pharmacodynamic-disease progression model for effects of anakinra in Lewis rats with collagen-induced arthritis. *J Pharmacokinet Pharmacodyn* **38:**769-786.

Lon HK, Liu D, DuBois DC, Almon RR, and Jusko WJ (2013) Modeling pharmacokinetics/pharmacodynamics of abatacept and disease progression in collagen-induced arthritic rats: a population approach. *J Pharmacokinet Pharmacodyn* **40:**701-712.

Lon HK, Liu D, Zhang Q, DuBois DC, Almon RR, and Jusko WJ (2011) Pharmacokinetic-pharmacodynamic disease progression model for effect of etanercept in Lewis rats with collagen-induced arthritis. *Pharm Res* **28:**1622-1630.

McInnes IB and Schett G (2011) The pathogenesis of rheumatoid arthritis. *N Engl J Med* **365:**2205-2219.

Miners JO, Coulter S, Tukey RH, Veronese ME, and Birkett DJ (1996) Cytochromes P450, 1A2, and 2C9 are responsible for the human hepatic O-demethylation of R- and S-naproxen. *Biochem Pharmacol* **51:**1003-1008.

Mortensen A, Jensen EB, Petersen PB, Husted S, and Andreasen F (1979) The determination of naproxen by spectrofluorometry and its binding to serum proteins. *Acta Pharmacol Toxicol (Copenh)* **44:**277-283.

Netter P, Bannwarth B, and Royer-Morrot MJ (1989) Recent findings on the pharmacokinetics of non-steroidal anti-inflammatory drugs in synovial fluid. *Clin Pharmacokinet* **17:**145-162.

Post TM, Freijer JI, DeJongh J, and Danhof M (2005) Disease system analysis: basic disease progression models in degenerative disease. *Pharm Res* **22:**1038-1049.

Poulin P (2015) A paradigm shift in pharmacokinetic-pharmacodynamic (PKPD) modeling: rule of thumb

for estimating free drug level in tissue compared with plasma to guide drug design. *J Pharm Sci*

104:2359-2368.

Renton KW (2005) Regulation of drug metabolism and disposition during inflammation and infection.

Expert Opin Drug Metab Toxicol **1:**629-640.

Ricciotti E and FitzGerald GA (2011) Prostaglandins and inflammation. *Arterioscler Thromb Vasc Biol*

31:986-1000.

Shah DK and Betts AM (2012) Towards a platform PBPK model to characterize the plasma and tissue

disposition of monoclonal antibodies in preclinical species and human. *J Pharmacokinet*

Pharmacodyn **39:**67-86.

Slaviero KA, Clarke SJ, and Rivory LP (2003) Inflammatory response: an unrecognised source of

variability in the pharmacokinetics and pharmacodynamics of cancer chemotherapy. *Lancet Oncol*

4:224-232.

Sokka T, Toloza S, Cutolo M, Kautiainen H, Makinen H, Gogus F, Skakic V, Badsha H, Peets T,

Baranauskaite A, Geher P, Ujfalussy I, Skopouli FN, Mavrommati M, Alten R, Pohl C, Sibilia J,

Stancati A, Salaffi F, Romanowski W, Zarowny-Wierzbinska D, Henrohn D, Bresnihan B,

Minnock P, Knudsen LS, Jacobs JW, Calvo-Alen J, Lazovskis J, Pinheiro Gda R, Karateev D,

Andersone D, Rexhepi S, Yazici Y, Pincus T, and Group Q-R (2009) Women, men, and rheumatoid

arthritis: analyses of disease activity, disease characteristics, and treatments in the QUEST-RA

study. *Arthritis Res Ther* **11:**R7.

Stuart JM, Cremer MA, Townes AS, and Kang AH (1982) Type II collagen-induced arthritis in rats. Passive

transfer with serum and evidence that IgG anticollagen antibodies can cause arthritis. *J Exp Med*

155:1-16.

Symmons DP (2002) Epidemiology of rheumatoid arthritis: determinants of onset, persistence and outcome.

Best Pract Res Clin Rheumatol **16:**707-722.

DMD # 74526

Takeshita M, Sugita T, and Takata I (1997) Pathological evaluation of effect of anti-rheumatic drugs on type II collagen-induced arthritis in Lewis rats. *Exp Anim* **46:**165-169.

van den Ouweland FA, Franssen MJ, van de Putte LB, Tan Y, van Ginneken CA, and Gribnau FW (1987) Naproxen pharmacokinetics in patients with rheumatoid arthritis during active polyarticular inflammation. *Br J Clin Pharmacol* **23:**189-193.

van Vollenhoven RF (2009) Sex differences in rheumatoid arthritis: more than meets the eye. *BMC Med* **7:**12.

Van Vollenhoven RF and McGuire JL (1994) Estrogen, progesterone, and testosterone: can they be used to treat autoimmune diseases? *Cleve Clin J Med* **61:**276-284.

Vane JR (1971) Inhibition of prostaglandin synthesis as a mechanism of action for aspirin-like drugs. *Nat New Biol* **231:**232-235.

Wanwimolruk S, Brooks PM, and Birkett DJ (1983) Protein binding of non-steroidal anti-inflammatory drugs in plasma and synovial fluid of arthritic patients. *Br J Clin Pharmacol* **15:**91-94.

Watson DJ, Rhodes T, Cai B, and Guess HA (2002) Lower risk of thromboembolic cardiovascular events with naproxen among patients with rheumatoid arthritis. *Arch Intern Med* **162:**1105-1110.

Footnotes

Figure Legends

Figure 1. Scheme of the mPBPK/PD/DIS model for pharmacokinetics and effects of NPX on paw edema in CIA rats. Parameters are defined in the text and Tables 1 and 2.

Figure 2. Model fittings of NPX plasma concentration versus time profiles (A and B) and fitted total and unbound NPX concentrations in plasma (solid lines) and ISF (dashed lines) (C to F) in female (left panels) and male (right panels) arthritic rats that received 50 mg/kg IP doses of NPX. Symbols are total plasma concentration measurements and curves depict model fittings or predictions. The embedded figure is the comparison of unbound ISF NPX concentrations in CIA females (dashed line) and males (solid line).

Figure 3. Predicted (solid curves) and literature-reported (symbols) total NPX concentrations in plasma (closed circles) and implanted sponge exudate fluid (ISF, open circles) versus time after oral administration of 10 mg/kg NPX to female rats (from Doherty et al, 1977) and bolus IP injection of 2.5, 10 and 25 mg/kg NPX to male rats (from Huntjens et al, 2006).

Figure 4. Disease progression of paw edema in female (upper panels) and male (lower panels) arthritic rats (n=4) after no drug (closed circles) and 50 mg/kg of NPX (open circles); time courses of paw volumes in male and female healthy rats (n=3) (closed triangles). Lines are model fittings of all data jointly yielding parameters listed in Table 2.

DMD # 74526

Table 1

Pharmacokinetic parameter estimates for NPX in healthy and CIA rats after IP administration

Parameter (units)	Definition	Estimates	CV%
k_a (1/h)	Absorption rate constant	0.98	8.3
f_d	Fraction of cardiac plasma flow	0.15	12.9
$CL_{Arthritic}$ (mL/h/kg)	Unbound plasma clearance in arthritic rats	1438	3.2
$CL_{Healthy}$ (mL/h/kg)	Unbound plasma clearance in healthy rats	1968	5.3
V_p (mL/kg)	Plasma volume	32.36 [a]	Fixed
V_t (mL/kg)	ISF volume	173.93 [a]	Fixed
Q_{co} (mL/h/kg)	Cardiac plasma flow	7650 [a]	Fixed

[a] Physiological parameter values obtained from (Shah and Betts, 2012).

25

Table 2

Pharmacodynamic parameter estimates for unbound ISF effects of NPX in healthy and CIA rats

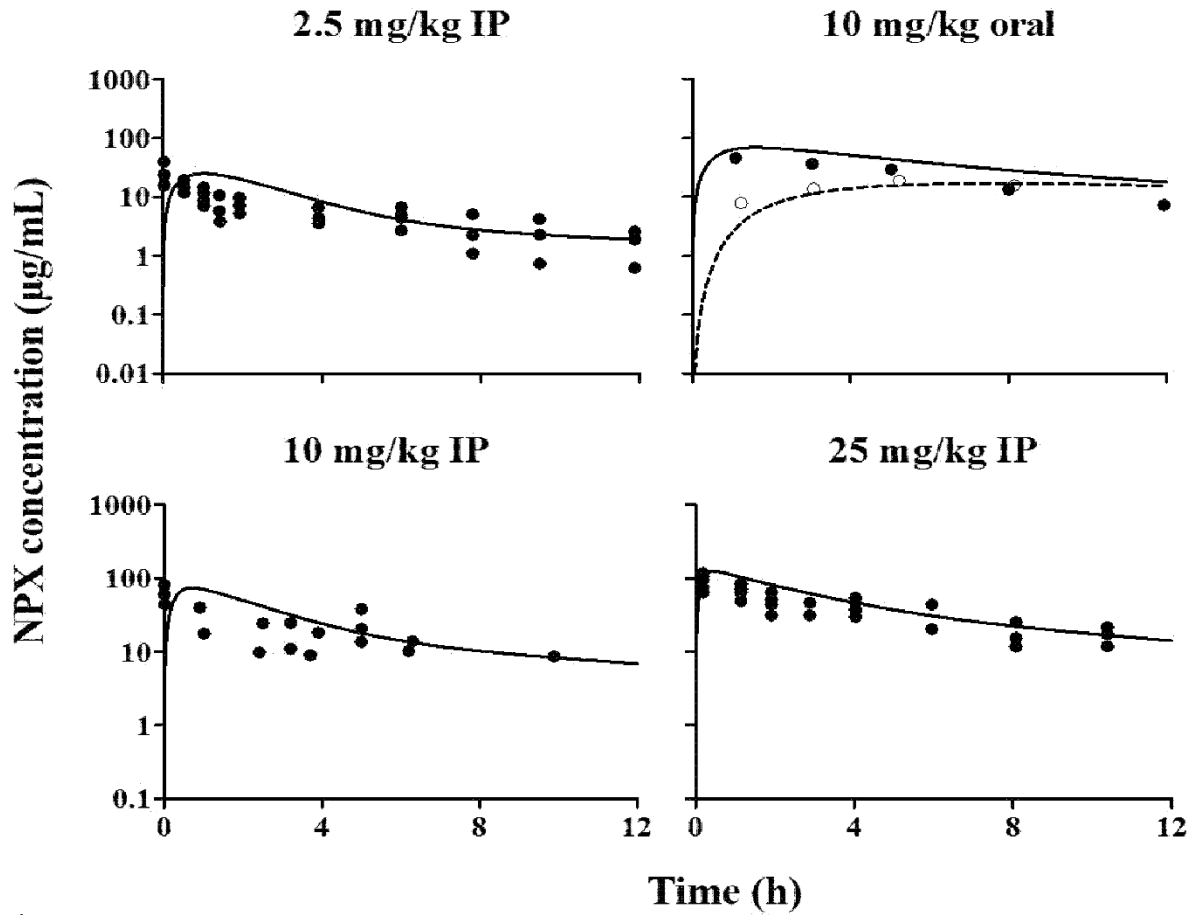| Parameter (units)	Definition	Estimates (CV%)	
		Females	Males
t_{onset} (h)	Time of disease onset	289 (1.07)	308 (0.5)
k_{out} (1/h)	Loss of edema rate constant	0.013 (41.3)	0.007 (20.6)
k_{deg} (1/h)	Loss of production rate constant	0.001 (29.0)	0.001 (16.6)
k_g (1/h)	Natural growth rate constant	0.003 (33.8)	0.002 (41.8)
I_{max}	Maximum inhibition on production of paw edema	0.75 (40.1)	1.0 (Fixed)
IC_{50} (μg/mL)	Unbound NPX concentration at 50% maximum inhibition	0.221 (56.4)	0.136 (45.9)
Paw_{ss} (mm^2)	Paw size at steady-state	70.2 (4.6)	102.2 (7.9)
$k_{in0,c}$ (mm^2/h)	Disease production rate constant at t_{onset} for control group	2.21 (24.6)	1.36 (12.0)
$Paw_{0,c}$ (mm^2)	Paw size on day 0 for control group	58.92 (1.6)	73.49 (1.8)
$k_{in0,t}$ (mm^2/h)	Disease production rate constant at t_{onset} for treatment group	2.31 (23.3)	1.44 (11.6)
$Paw_{0,t}$ (mm^2)	Paw size on day 0 for treatment group	59.99 (1.6)	76.02 (1.6)
$Paw_{0,ng}$ (mm^2)	Paw size on day 0 for natural growth group	50.38 (2.9)	77.43 (1.8)

26
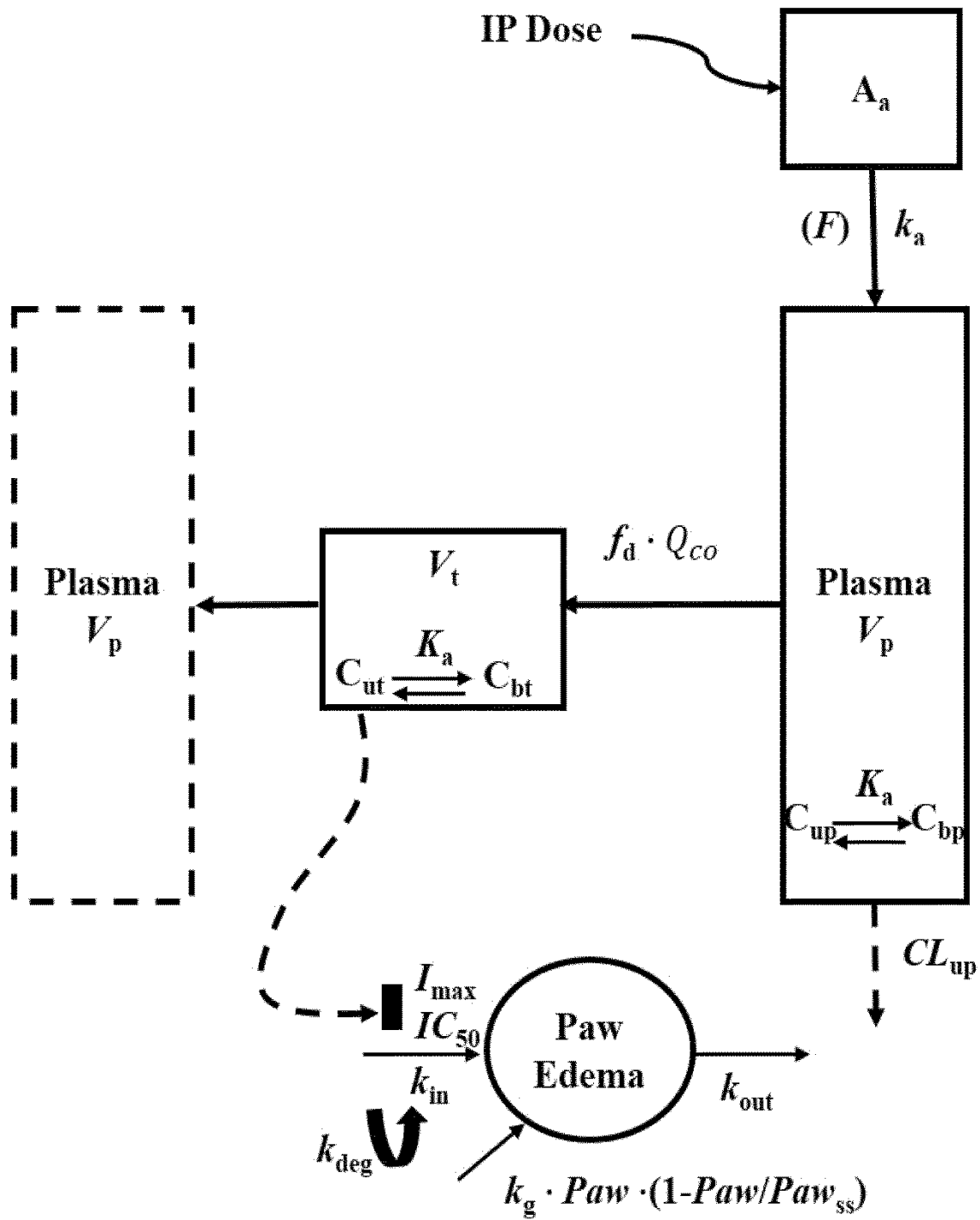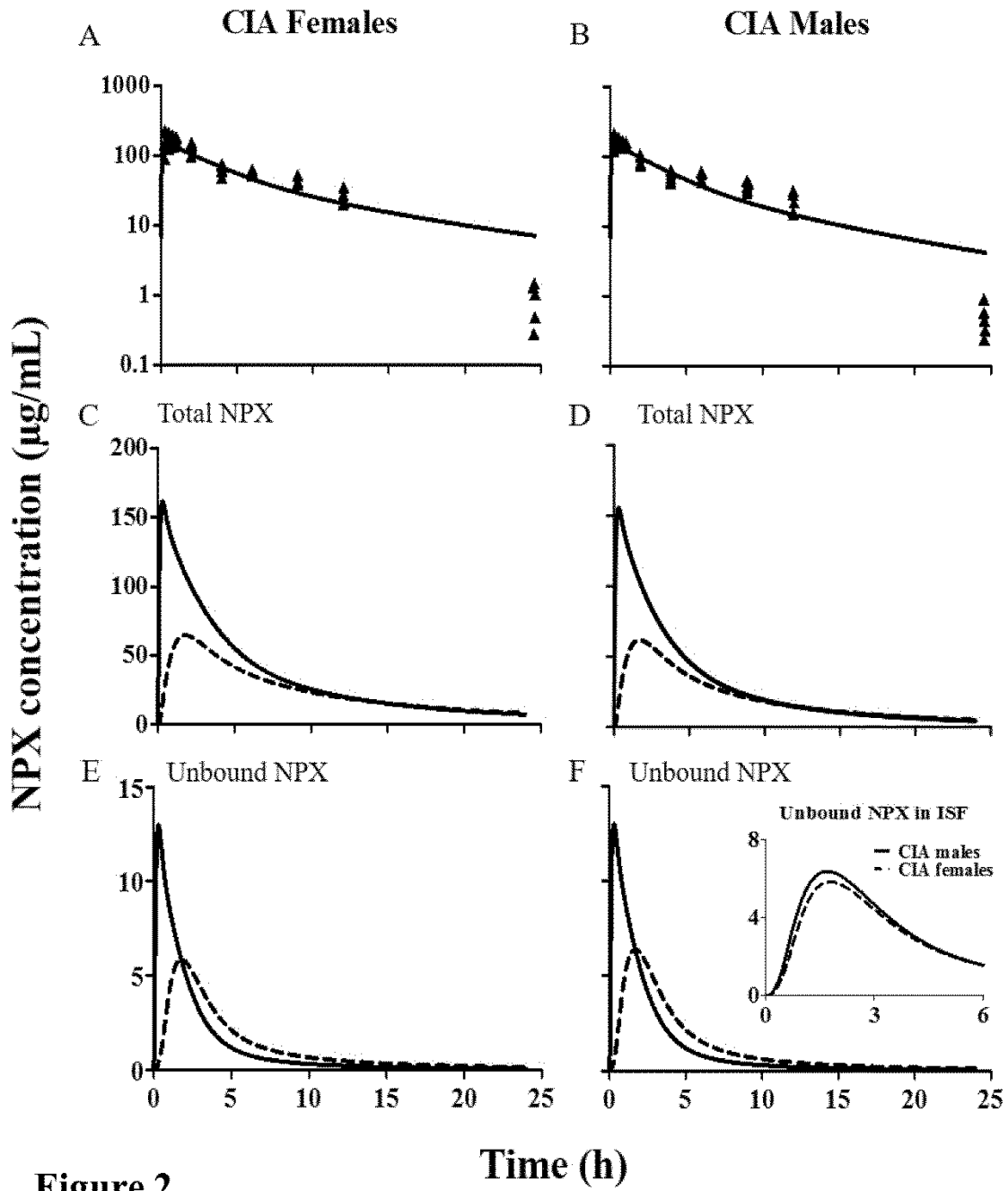
Figure 1.

Figure 2.

Figure 3.

Figure 4.